Technical Notes

TECHNICAL NOTES are short manuscripts describing new developments or important results of a preliminary nature. These Notes cannot exceed 6 manuscript pages and 3 figures; a page of text may be substituted for a figure and vice versa. After informal review by the editors, they may be published within a few months of the date of receipt. Style requirements are the same as for regular contributions (see inside back cover).

Turbulence Measurements in a Ducted Coaxial Flow

RICHARD A. KULIK,* JACK J. LEITHEM,† AND HERBERT WEINSTEIN‡
Illinois Institute of Technology, Chicago, Ill.

Nomenclature

r	=	radius variable
r_0	=	inner stream initial radius
u	=	mean velocity
u_0	=	maximum initial velocity
u'	=	rms axial turbulence intensity
v'	=	rms radial turbulence intensity
$[u'v'/(u')(v')]$	=	correlation coefficient between u' and v'
z	=	axial distance variable

Introduction

THE mixing of turbulent ducted coaxial streams has been investigated to a great extent recently because of interest in such areas as thrust augmentation devices and supersonic combustion chambers. Most of the experimental investigations, however, considered the case with the inner stream moving faster than the outer one and reported only mean velocity data. This investigation was directed toward the study of the feasibility of gas core nuclear rockets and had as its object to examine ducted coaxial flows with the outer stream moving faster than the inner stream.[1] Mean values of axial velocity and the rms values of the fluctuations in axial and radial velocities and the correlation between them were determined throughout the flowfield. Both the inner and outer stream fluids were air.

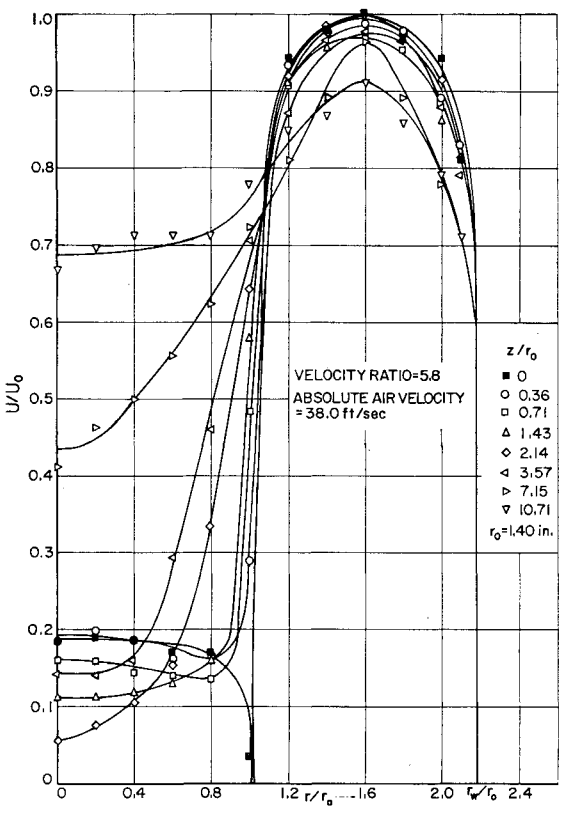

Fig. 1 Mean velocities.

Experimental Technique

Apparatus

The tunnel used in this study consisted of three sections: 1) a square reducing entrance section, 2) a 3-ft length of 6 in. i.d. sheet metal duct in which a 2.8-in. i.d. inner aluminum tube was mounted coaxially, and 3) a 4-ft length of 6-in. i.d. Lucite duct, the lower foot of which was stacked with cardboard honeycomb to prevent feedback of any exit effects such as swirling of the fluid. The aluminum inner tube extended 6 in. down into the outer Lucite tube so that there was a $2\frac{1}{2}$-ft turbulent mixing text section. (See Ref. 1 for a complete description.)

The inner air stream was pressure fed in the top end of the aluminum tube through a fritted glass disk to achieve a uniform flow. The outside of the lower open end of this tube was machine tapered from 0.082 in. to 0.005 in. over an 18 in. length. This provided a relatively smooth transition from annular to mixed flow. To reduce the turbulence and tem-

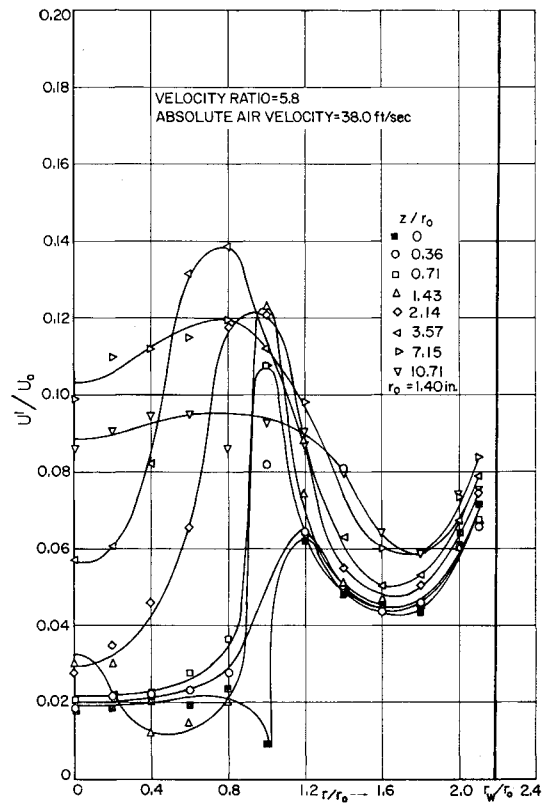

Fig. 2 Axial turbulent intensities.

Received April 29, 1970. The complete support of this work was provided by NASA, under Grant NGR 14-004-008 (041) and is gratefully acknowledged.

* Research Assistant, Department of Chemical Engineering.
† Development Engineer; present address Universal Oil Products, Des Plaines, Illinois.
‡ Associate Professor, Department of Chemical Engineering.

perature effects of the blower, the outer air stream was sucked through the test section instead of being blown through.

Data was taken with two channels of Thermo-Systems Inc. model 1000A constant temperature hot wire anemometers. Single hot film sensors were used to find mean velocities and axial rms velocity fluctuations while a cross probe arrangement was used to measure the $u'v'$ correlation as well as the radial rms velocity fluctuations.

Results and Discussion

Figures 1–4 give, respectively, mean velocity profiles, axial turbulence intensity profiles, radial turbulence intensity profiles, and profiles of the correlation of u' and v' for several axial stations. From these figures several zones of flow can be seen. At the near axial stations, or initial region, three zones are visible. The first zone extends from the centerline to $r/r_0 < 0.8$. This zone corresponds to what is sometimes called the potential core region or the undisturbed inner stream region. In this zone the inner stream loses its pipe flow properties and merges with the outer stream. The $u'v'$ correlation is positive, u' and v' do not vary much, and the velocity profile changes from that of a pipe flow to that of the central portion of a mixing region. The second zone is between $0.8<r/r_0<1.6$, which contains the growing mixing region between the streams. Here, the $u'v'$ correlation is negative, u' and v' show maxima, and the mean velocity profiles show inflection points and large gradients. u' is about 50% larger than v' here as it also appears to be in the other zones. The ratio of u' to v', however, does not appear to be as great as it does for unconfined coaxial flows.[2] The third zone, $1.6<r/r_0<$wall, is the wall region where the behavior of the flow closely approximates that of the wall region in a turbulent pipe flow. The correlation, u' and v' all rise rapidly approaching the wall, peak, and then fall to a zero value at the wall. This zone does not change much over the whole length of the field considered. The initial region as seen from the mean velocity profile plot of Fig. 1 extends to approximately

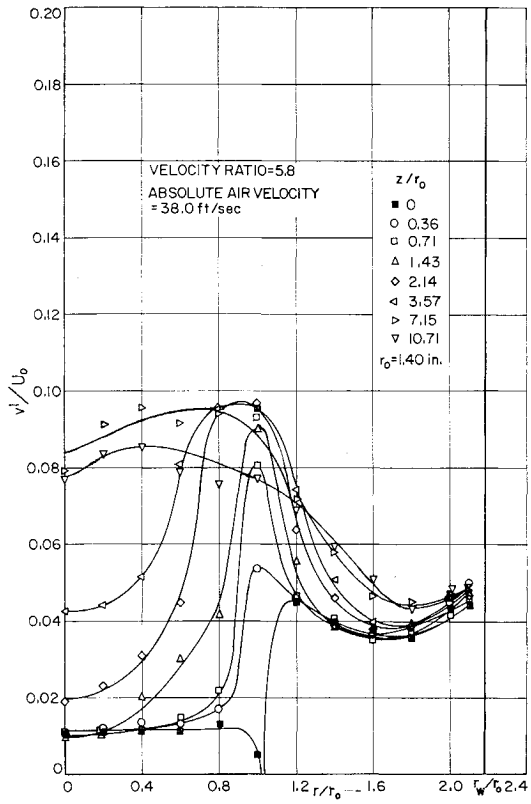

Fig. 3 Radial turbulent intensities.

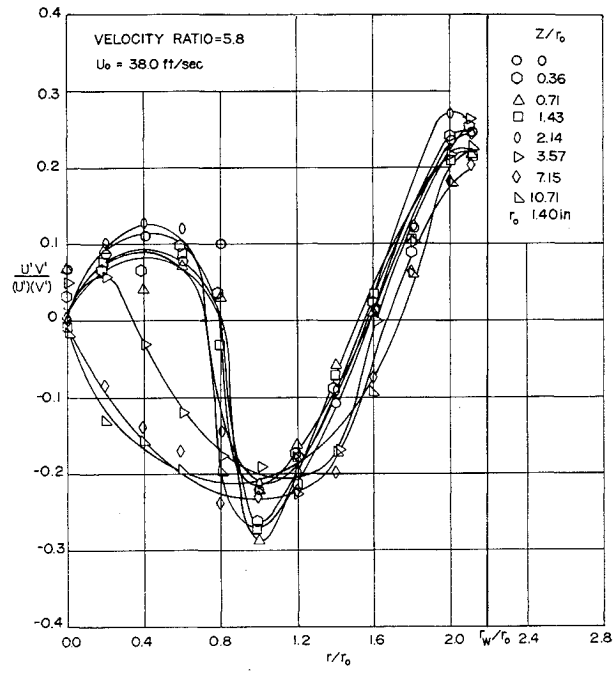

Fig. 4 Cross-correlation coefficient.

$z/r_0 = 1.2$. However, the initial region as seen from Fig. 4, the $u'v'$ profile plot, extends to $z/r_0 = 4$.

Further downstream, only two zones of flow are visible. There is a mixing region, $r/r_0<1.6$, and a wall region, $r/r_0>1.6$. The mixing region profiles are all similar in shape to those of a free mixing region until r/r_0 approaches 1.6. Then the effects of the velocity maximum are felt. The correlation goes through zero and the intensities through minima. The inflection point in the $u'v'$ curve coincides approximately with its zero point. The downstream wall region is essentially unchanged from the initial region.

It should be pointed out that the largest errors in measurement of the correlation occur near and at the zero values and that the axial location of these values are in doubt and cannot be cross-plotted accurately. However, Fig. 5 is a cross-plot of the locations of the zeroes of $u'v'$ from Fig. 4, and the zeroes of $\partial u/\partial r$ from Figure 1. In the so-called undisturbed inner stream region the $\partial u/\partial r = 0$ curve starts just inside the inner duct wall and reaches the centerline very shortly downstream, at approximately $z/r_0 = 1.2$. However, the $u'v' = 0$ curve does not reach the centerline until $z/r_0 = 4$. The region between these two curves is characterized by a positive value of $\partial u/\partial z$. A region where $u'v'$ and $\partial u/\partial r$ have the same sign

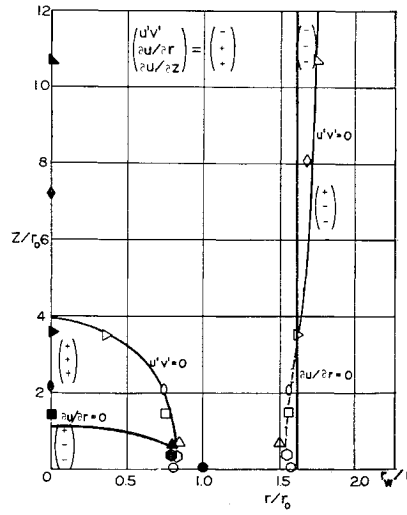

Fig. 5 Zeroes of the cross-correlation and velocity gradient.

has been called a region of opposing shear.[4] This region of opposing shear is apparently dominated by the concentrated vortex sheet between $1 \leq r/r_0 \leq 1.6$ which induces a velocity component upstream.[3] The region between the zeroes of $u'v'$ and $\partial u/\partial r$ near $r/r_0 = 1.6$ and $z/r_0 > 5$ is also a region of opposing shear and is similar in nature to the region of opposing shear found in wall jets.[4] This second region of opposing shear is one in which $\partial u/\partial z$ is negative. In summary, for this axisymmetric flowfield, there appear to be two regions of opposing shear (where $u'v'$ and $\partial u/\partial r$ have the same sign) one in which the sign of $\partial u/\partial z$ is negative and one in which it is positive.

References

[1] Leithem, J. J., Kulik, R. A., and Weinstein, H., "Turbulence in the Mixing Region Between Ducted Coaxial Streams," CR-1335, July 1969, NASA.

[2] Zawacki, T. S. and Weinstein, H., "Experimental Investigation of Turbulence in the Mixing Region Between Coaxial Streams," CR-959, Feb. 1968, NASA.

[3] Rozenman, T. and Weinstein, H., "Recirculation Patterns in the Initial Region of Coaxial Jets," CR-1595, May 1970, NASA.

[4] Eskinazi, S. and Erian, F. F., "Energy Reversal in Turbulent Flows," *The Physics of Fluids*, Vol. 12, No. 10, p. 1988, 1969.

A Recurrence Relationship for Parameter Estimation via Method of Quasi-Linearization and its Connection with Kalman Filtering

ROBERT T. N. CHEN*
Cornell Aeronautical Laboratory, Buffalo, N. Y.

Introduction

BEFORE the age of high-speed digital computers,[1] the estimation of parameters and state for nonlinear dynamical systems had been a challenging and difficult task. Although this task has been made somewhat easier with the aid of high-speed computers, an ultimate solution is still out of reach. Goodwin[2] recently compared several off-line deterministic, measurement-error methods for the parameter and state estimation of nonlinear systems. These techniques consist of the simplified gradient method,[4] conjugate gradient methods,[6,7] Goodwin's modified Newton procedures,[3,5] and the quasi-linearization method.[13,14] For the specific nonlinear system Goodwin considered, the results showed that the rate of convergence of the modified Newton methods and the method of quasilinearization are superior. Experience[15,16] gained in the identification of the stability and control parameters of aircraft has also indicated that the method of quasi-linearization is better than the gradient methods.

The success experienced in state estimation using an extended Kalman filtering[7,8] method in aerospace applications in the early sixties has encouraged broader applications in industry, particularly in chemical engineering.[17,18] However, in the absence of statistical information concerning the measurement noise and the process noise, the results obtained from the deterministic, least-square viewpoint would seem to have more engineering appeal. Detchmendy and Sridhar[9] applied the technique of invariant imbedding[10] and obtained a sequential algorithm for the state and parameter estimation of nonlinear systems with measurement and process noise. This generalized the results of Bellman and others[10] which treated only the measurements error. However, it is interesting to note that Detchmendy's algorithm is identical to the extended Kalman filtering if the output is a linear operation on the state and weighting matrices are chosen to be the inverse of the corresponding covariance matrices of the noise. In view of the popularity of the quasilinearization and Kalman filtering methods, it seems desirable to establish a relationship between these two methods. With the assumption that process noise is absent, the relationship between the two methods is established in this Note.

Received November 18, 1969; revision received April 30, 1970. This work was partially supported by the Naval Air Systems Command under Contract N00019-69-C-0534. The author gratefully acknowledges the helpful discussions he had with E. Rynaski, R. Harper, and J. Schuler of Cornell Aeronautical Laboratory, and J. Tyler of Analytical Mechanic Associates Inc. during the course of this work.

* Research Engineer, Flight Research Department.

Method of Quasi-Linearization

This method is also referred to as Gauss-Newton procedure, parameter-influence-coefficient method, "modified" Newton-Raphson method, etc. It is concerned with the following problem.

Given a nonlinear dynamic system along with its measurement system

$$\dot{x} = f(x,p,t),\ x(t_0) = \alpha \tag{1a}$$

$$y = g(x,t) + v \tag{1b}$$

where x is the state vector (n vector); p is the parameter vector (r vector); y is the output vector (m vector); f and g are vector functions of appropriate dimension; and v is the error vector of the measurements.

Find an estimate of the parameter vector p and initial conditions α which minimize

$$J = \frac{1}{2}\int_{t_0}^{t_f} [y(t) - g(x,t)]^T W [y(t) - g(x,t)]dt \tag{1c}$$

where T denotes transposition, t_f the final time, and W is a positive definite symmetrical weighting matrix.

The method of quasi-linearization[13,15] begins with the linearizations of the trajectory and the output about the old estimates $\hat{p}$ and $\hat{\alpha}$;

$$x(\hat{\alpha} + \Delta\alpha, \hat{p} + \Delta p) \approx x(\hat{\alpha},\hat{p}) + \begin{bmatrix} \frac{\partial x}{\partial \alpha}, & \frac{\partial x}{\partial p} \end{bmatrix} \begin{bmatrix} \Delta\alpha \\ \Delta p \end{bmatrix} \tag{2}$$

$$g(x,t) \approx g[x(\hat{\alpha},\hat{p}),t] + \frac{\partial g}{\partial x} \begin{bmatrix} \frac{\partial x}{\partial \alpha}, & \frac{\partial x}{\partial p} \end{bmatrix} \begin{bmatrix} \Delta\alpha \\ \Delta p \end{bmatrix} \tag{3}$$

The sensitivity matrices $\partial x/\partial\alpha$ and $\partial x/\partial p$ are obtained from the solution of the following set of linear time-varying differential equations:

$$\frac{d}{dt}\left(\frac{\partial x}{\partial \alpha}\right) = \left(\frac{\partial f}{\partial x}\right)\left(\frac{\partial x}{\partial \alpha}\right),\ \frac{\partial x}{\partial \alpha}(0) = I_n \tag{4a}$$

$$\frac{d}{dt}\left(\frac{\partial x}{\partial p}\right) = \left(\frac{\partial f}{\partial x}\right)\left(\frac{\partial x}{\partial p}\right) + \frac{\partial f}{\partial p},\ \frac{\partial x}{\partial p}(0) = 0 \tag{4b}$$

where I_n is the nth order identity matrix.

Equating the gradient $\nabla_p{}^*J$ [evaluated at the new estimate p^*, where $p^* = \mathrm{col}(\alpha^T, p^T)$] to zero yields a new estimate

$$\hat{p}_{\text{new}}{}^* = \hat{p}_{\text{old}}{}^* + \Delta p^*$$

$$\Delta p^* = \left\{\int_{t_0}^{t_f} \begin{bmatrix} \partial x^T/\partial\alpha \\ \partial x^T/\partial p \end{bmatrix} \left(\frac{\partial g}{\partial x}\right)^T W \left(\frac{\partial g}{\partial x}\right)\left(\frac{\partial x}{\partial \alpha} \vdots \frac{\partial x}{\partial p}\right) dt\right\}^{-1} \times \int_{t_0}^{t_f} \begin{bmatrix} \partial x^T/\partial\alpha \\ \partial x^T/\partial p \end{bmatrix} \left(\frac{\partial g}{\partial x}\right)^T W [y(t) - g(\hat{x},t)]dt \tag{5}$$

where the Jacobian matrices $\partial f/\partial x$, $\partial f/\partial p$, $\partial g/\partial x$, and the computed output $g(\hat{x},t)$ are evaluated at the old estimate $p_{\text{old}}{}^*$.